Biotransformation and detoxification of selenite by microbial biogenesis of selenium-sulfur nanoparticles

Vogel, M.; Fischer, S.; Maffert, A.; Hübner, R.; Scheinost, A.; Franzen, C.; Steudtner, R.;

Originally published:

October 2017

Journal of Hazardous Materials 344(2018), 749-757

DOI: https://doi.org/10.1016/j.jhazmat.2017.10.034

Graphical abstract

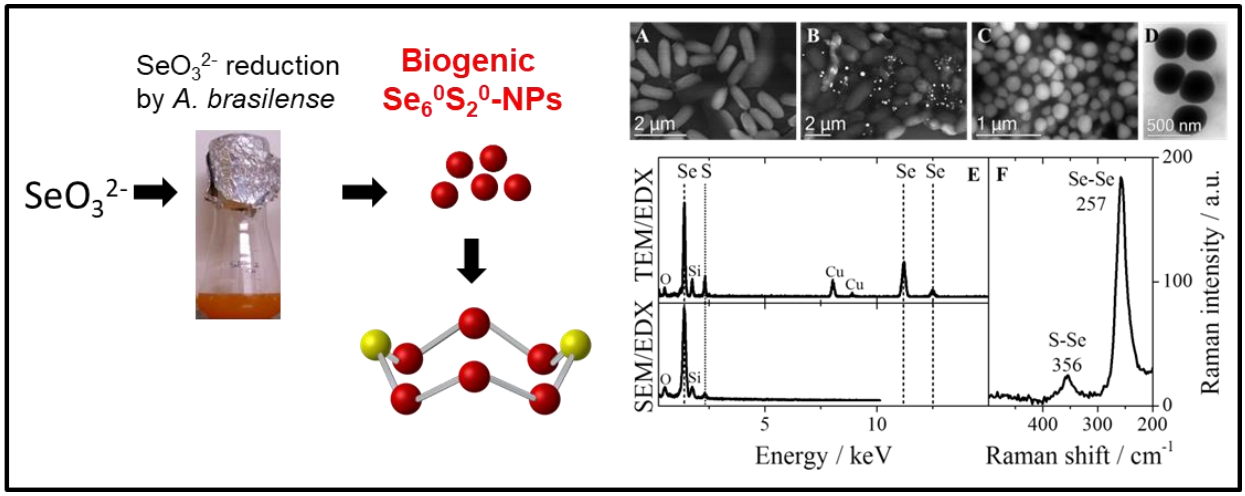

Highlights

- *A. brasilense* is able to efficiently reduce toxic selenite to Se^0S^0-nanoparticles
- Reduction was also possible in environmental waters supplemented with selenite
- Biogenic nanoparticles are $Se_{8-n}S_n$ structured spheres, most likely Se_6S_2
- Se^0S^0- nanoparticles occur extracellularly with an average size of 400 nm
- Se^0S^0-nanoparticles form a (destabilized) colloidal suspension (ζ-potential – 18 mV)

Biotransformation and detoxification of selenite by microbial biogenesis of selenium-sulfur nanoparticles

M. Vogel[1,3], S. Fischer[1], A. Maffert[1,3], R. Hübner[2], A. Scheinost[1], C. Franzen[1], R. Steudtner[1*]

[1]Helmholtz-Zentrum Dresden-Rossendorf e.V., Institute of Resource Ecology, Bautzner Landstrasse 400, D-01328 Dresden / Germany

[2]Helmholtz-Zentrum Dresden-Rossendorf e.V., Institute of Ion-Beam Physics and Materials Research, Bautzner Landstrasse 400, D-01328 Dresden / Germany

[3]Helmholtz-Zentrum Dresden-Rossendorf e.V., Helmholtz Institute Freiberg for Resource Technology, Bautzner Landstrasse 400, D-01328 Dresden / Germany

[*]Corresponding author:

Dr. Robin Steudtner, Helmholtz-Zentrum Dresden-Rossendorf e.V., Institute of Resource Ecology, Bautzner Landstrasse 400, D-01328 Dresden / Germany

E-mail: r.steudtner@hzdr.de

Telephone: +49 351 260 2895,

Fax number: +49 351 260 3553

Email addresses:

m.vogel@hzdr.de, sarah.fischer@hzdr.de, a.maffert@biconex.de, r.huebner@hzdr.de, a.scheinost@esrf.fr, c.franzen@hzdr.de, r.steudtner@hzdr.de

Abstract

This study combines the interaction between the toxic oxyanions selenite and selenate and the plant growth promoting bacterium *Azospirillum brasilense* with a comprehensive characterization of the formed selenium particles. As selenium is an essential trace element, but also toxic in high concentrations, its state of occurrence in nature is of major concern. Growth of the bacterium was affected by selenite (1 – 5 mM) only, observable as a prolonged growth lag-phase of 3 days. Subsequently, selenite reduction occurred under aerobic conditions resulting in extracellularly formed insoluble Se^0 particles. Complementary studies by microscopic and spectroscopic techniques revealed the particles to be homogeneous and stable $Se_{8-n}S_n$ structured spheres with an average size of 400 nm and highly negative surface charge of -18 mV in the neutral pH range. As this is the first study showing *Azospirillum brasilense* being able to biotransform selenite to selenium particles containing a certain amount of sulfur, even if environmental waters supplemented with selenite were used, they may significantly contribute to the biogeochemical cycling of both elements in soil as well as to their soil-plant transfer. Therefore, microbial biotransformation of selenite under certain circumstances may be used for various bio-remediation and bio-technological applications.

Keywords:

biogenic selenium nanoparticles, *Azospirillum brasilense*, selenite reduction, bioremediation, sulfur nanoparticles

1. Introduction

In the present time, water contamination by substances such as heavy metals, toxic organics, radionuclides or nanoparticles poses an increasing problem of global concern, especially in drinking water treatment and in the purification of process water from many industrial applications [1]. For the improvement of water quality in the contaminated streams, detailed knowledge on chemical, biological and physical interaction of these noxious chemicals are mandatory. With respect to synthetic submicron- or nanoparticles in water matrices, respective knowledge is still limited. In this context, selenium with its ambivalent biologic characteristics is an especially challenging case. For living organisms, selenium is a key trace element, but the healthy level between selenium deficiency (< 40 µg/day) and acute selenium poisoning (> 400 µg/day) is rather narrow [2].

Selenium can exist in different oxidation states. The oxyanions selenate [SeO_4^{2-}] and selenite [SeO_3^{2-}] represent soluble species in aqueous media, whereas the reduced species Se^0 and Se^{2-} form mainly colloidal particles or hardly soluble precipitates [3]. Chemical equilibrium speciation information on selenium oxidation state are challenging, discussed and summarized in “Chemical Thermodynamics of Selenium.” by OECD Nuclear Energy Agency [4]. The standard electrode potential of the redox couples are given in the supplementary information. Selenium is ubiquitous in natural environments (e.g. associated with various sulfide ores of copper, silver, lead, mercury and uranium) and has also anthropogenic origins, e.g. coal burning for power generation, agricultural irrigation of seleniferous soils [1, 5-8]. Besides the potential chemotoxicity, the isotope ^{79}Se as a fission product with a long half-life (~3.27×10^5 years [9]) is present in spent nuclear fuel. Several national reports for the long-term

safety assessment of high-level nuclear waste disposals show that ^{79}Se is one of the radionuclides that dominate the long-term dose rate [10, 11].

These days, selenium becomes more and more important for technological applications, in consequence of its photoelectric and semiconducting properties [5]. Respective releases from industrial process waters and wastes have to be considered, too. Eventually, to understand the cycling of selenium in the environment is of great importance for the well-being of humans as well as for saving resources.

One possible way to address these hazards is to transform toxic soluble selenium species into insoluble selenium species like nanoparticles promoting their technological separation by sedimentation, coagulation and filtration.

Reactions between selenium and microorganisms can significantly influence the selenium oxidation state and therefore the transport through geological environment. Recently, many investigations have shown that bacteria are able to form Se^0 particles under anaerobic as well as aerobic conditions (e.g. *Geobacter sulfurreducens*, *Veillonella atypical*, *Bacillus subtilis*, *Bacillus cereus*, *Shewanella putrefaciens*, *Agrobacterium* sp., *Pseudomonas aeruginosa*, *Stenotrophomonas maltophilia*) [12-19].

In addition to the better separation of particulate selenium from water, nanoparticles attract special interest since their properties usually differ significantly from those of the bulk material. Especially Se^0 nanoparticles have various attractive features, like higher biological activity [20], lower toxicity [21, 22] and larger surface area [23]. They have novel *in vitro* and *in vivo* antioxidant activities and provide new pathways for medical application like cancer treatment as well as anti-bacterial coating material [24-28]. In the photovoltaic and semiconductor industry Se^0 nanoparticles are used because of their high particle dispersion and unique electrical and optical properties.

Other practical applications in the field of nanotechnology are under development [23, 27, 29] Finally, recent studies have shown Se^0 nanoparticles being good adsorbents for heavy metals such as Zn, Hg or Cu [29-31]

In the present study, the interaction of SeO_3^{2-} and SeO_4^{2-} with the plant growth promoting rhizobacterium *Azospirillum brasilense* was investigated, which were reported to have the ability to form Se^0 nanoparticles [32, 33] earlier. As this bacterium might be used for biological fertilization also in regions with heavily selenite-loaded soils, its influence on the transfer of the toxic selenium oxyanion as well as the reduction potential needs to be further elucidated. As it was reported that *Azospirillum* forms the Se^0 particles mainly inside the cells [32, 33], this bacteria might be helpful to prevent migration of (radio)toxic selenium through soil and water, as the selenium remains entrapped inside the biomass [34, 35]. Kamnev et al. [36] used *A. brasilense* to obtain extracellular Se nanoparticles, which were than further characterized by infrared spectroscopy and electron microscopy. In this study, after comparable growth experiments to Tugarova et al. [32, 33] special focus was set on the physico-chemical and structural characterization of the formed Se^0 particles, confirming results already reported, but revealing also some more profound and interesting new structural aspects on the Se particles. The formation of hardly soluble Se(0) particles during reduction of selenium oxyanions might be of interest for an industrial application. Moreover, if the Se^0 particles will be released from the biomass (e.g. cell death), the mobility of the selenium particles in the environment will be governed by their physico-chemical properties.

So in this study, the elemental selenium particles for further investigation were produced by *Azospirillum brasilense.* The process of microbial selenium reduction was tracked by inductively coupled plasma mass spectrometry (ICP-MS), hydride

generation atomic absorption spectrometry (HG-AAS) and light microscopy. Scanning and transmission electron microscopy (SEM and TEM) with energy dispersive X-ray (EDX) microanalysis, Raman spectroscopy, X-ray absorption spectroscopy (XAS) and UV/Vis spectroscopy (UV/Vis) as well as zeta potential measurements and photon correlation spectroscopy (PCS) were used to characterize the formed selenium particles.

2. Material and methods

2.1 Medium and growth conditions

Growth medium for *Azospirillum brasilense* (DSMZ 1843) was a malate-containing Azo-medium (DSMZ 2007). Medium components (yeast extract 0.05 g, K_2HPO_4 0.25 g, $FeSO_4 \cdot 7\ H_2O$ 0.01 g, $Na_2MoO_4 \cdot 2\ H_2O$ 1.00 mg, $MnSO_4 \cdot H_2O$ 2.00 mg, $MgSO_4 \cdot 7\ H_2O$ 0.20 g NaCl 0.10 g, $CaCl_2 \cdot 2\ H_2O$ 0.02 g, $(NH_4)_2SO_4$ 1.00 g, Biotin 0.10 mg) were solved in 950 ml distilled water and pH was adjusted to 7.1 before autoclaving. After sterilization 25 ml each of filter-sterilized 20% glucose and 20% Na-malate were added.

Cells were grown under aerobic conditions in liquid medium in flasks on a rotary shaker at 100 rpm at 30 °C.

2.2 Incubation with selenate and selenite

For growth experiments in the presence of selenate and selenite, pre-cultured cells were inoculated into 250 mL flasks containing 150 mL of Azo-medium reaching a starting optical density at 600 nm (OD_{600}) of 0.25. The different concentrations of selenite (1 mM to 5 mM) or selenate (1 mM) in the assay were obtained by addition of the required volume of stock solutions of 0.1 M $Na_2SeO_3 \cdot 5\ H_2O$ or 0.1 M Na_2SeO_4. Two replicates of each concentration were incubated as described above

and sampled at intervals. Samples were assayed for bacterial density, whole cell protein concentration, selenite and selenate.

2.3 Analysis

The optical density of the cell suspension was measured at 600 nm with a UV/Vis-spectrophotometer (Ultrospec 1000, Pharmacia Biotech). Additionally, cell growth was monitored by determination of whole cell protein concentration to overcome interference from Se particles in spectrophotometric measurement of optical cell density. Therefore, 2 mL of bacterial suspension were centrifuged first slowly for 10 min at 1000xg, to separate most of Se particles from bacterial cells, and then for 10 min at 10,000×g and washed twice with 0.1 M NaCl. The cell pellet was then suspended in 500 µL cell lysis buffer (NaCl 9 g/L, NaOH 12 g/L) and incubated for 10 min at 90 °C. Afterwards the suspension was cooled in an ice bath and centrifuged again. From the supernatant 50 µL were used for bicinchoninic acid (BCA) protein assay.

Selenite concentrations were determined using hydride generation atomic absorption spectrometry (HG-AAS) and total selenium concentration was measured by inductively coupled plasma mass spectrometry (ICP-MS). For this, bacteria and other particles were separated from medium by centrifugation at 10,000×g for 10 min.

Cells were separated from the Se particles by a modified protocol according to Oremland et al. [37]. Therefore the cell suspension was ultrasonicated at 100 W for 2 min and centrifuged at 1500×g for 30 min. The sediment was resuspended, ultrasonicated and centrifuged sequentially in 0.5 M NaCl, 0.5 M sucrose and in salt solution with pH 7.5 (NaCl 17.5 g/L, KCl 0.74 g/L, $MgSO_4 \cdot 7\ H_2O$ 12.3 g/L, Tris base 0.15 g/L). Cells were then lysed in 35 mL salt solution by the addition of 0.02 g

lysozyme and incubation for 19 h at room temperature. The lysed cells were washed away from the Se^0 particles by sequential centrifugation (9000×g, 15 min), resuspension, ultrasonication and incubation (2 h) in salt solution, 0.25 M NaOH, 0.1 M NaOH, 10 mM Na_2HPO_4 (pH 7.3) and deionized water. For characterization the cleaned Se^0-nanoparticles were resuspended in deionized water.

2.4 Electron microscopy with energy dispersive X-ray analysis

Samples for scanning electron microscopy (SEM) were either washed with PBS (NaCl 8 g/L, KCl 0.2 g/L, $NaHCO_3 \cdot 2\ H_2O$ 1,8 g/L, KH_2PO_4 0.24 g/L, pH 7.4), fixed with 2% glutaraldehyde for 1 h and washed with deionized water or just washed two times with deionized water before mounting aliquots of 5 µL on silicon wafers. The fixation procedure was carried out for a better visualization of the bacteria in presence of the formed nanoparticles. For transmission electron microscopy (TEM) of the Se^0 particle suspension, carbon-formvar-coated copper grids (Plano, Wetzlar, Germany) were used as sample support.

Scanning electron microscopy was performed using a S-4800 microscope (Hitachi) operated at an accelerating voltage of 10 kV. For qualitative chemical analysis of the Se nanoparticles, energy dispersive X-ray spectroscopy analysis was carried out by means of a conventional Si(Li) detector with S-UTW window (Oxford Instruments) attached to the SEM. Transmission electron microscopy investigations were performed with an image C_s-corrected Titan 80-300 microscope (FEI) at an accelerating voltage of 300 kV. Employing a Li-drifted silicon detector (EDAX) in STEM mode, EDX measurements were performed for qualitative chemical analysis.

2.5 Raman spectroscopy

Raman spectroscopic measurements of the Se^0 particle suspensions were carried out with a Raman microscope (HORIBA Jobin Yvon LabRAM Aramis Vis) using a HeNe-Laser (633 nm) with an output energy of 0.17 mW as light source.

2.6 Photon correlation spectroscopy

Photon correlation spectroscopy was carried out by a Nano Zetasizer (Malvern Instruments) with a laser beam of 633 nm, a scattering angle of 173°, and at 22°C. The ζ-potential and hydrodynamic diameter (HDD) were calculated by DTS software (Malvern Instrument) using electrophoretic mobility. The general purpose algorithm in the DTS software was used for calculating the size distribution.

2.7 X-ray absorption spectroscopy

For complementary chemical characterization of the formed selenium particles X-ray absorption spectroscopy (XAS) was applied. Selenium K-edge XANES (X-ray Absorption Near-Edge Structure) and EXAFS spectra were collected at the Rossendorf Beamline at ESRF (Grenoble, France). Further details on the sample preparation, experimental XAS setup and data analysis are compiled in Jordan et al. (2014) [38]. The XAS data were analyzed using the SIXpack [39] and WinXAS [40] program as application software and the theoretical phase and amplitude functions of the spectra were calculated with the FEFF 8.20 code [41] based on a references selenium red (nanoparticulate) (AcReDaS 00000059).

3. Results and discussion

3.1 Evaluation of reducing ability and growth of *Azospirillum brasilense* on selenite and selenate

To determine the reducing ability of *A. brasilense* for selenate and selenite, the bacterium was grown in the presence of 1 mM sodium selenate and sodium selenite, respectively. As shown in Figure 1A, selenate was not reduced by *A. brasilense*. The slight increase of selenate concentration over time can be attributed to evaporation of medium during incubation. The growth behavior of the cells in presence of toxic selenate was similar to control cell suspensions without selenium oxyanions in the medium (data not shown). As the growth of the bacterium at this selenate concentration was not affected it can be considered being non-toxic.

In contrast, toxic selenite was reduced by *A. brasilense* under aerobic conditions to non-toxic elemental red selenium particles which was indicated by a change in color of the cell suspension to orange-red compared to the slightly red of the control cell suspension. That the reduction of selenite is due to bacterial activity is concluded from results shown in Figure 1 and from control experiments with selenite in medium lacking bacteria (data not shown). Because of the selenite toxicity, growth of the bacteria was inhibited for two days. During this prolonged lag-phase, no selenite reduction or oxidation occurred. Shortly after the start of cell growth, selenite was reduced continuously. The higher biomass content at the end of the incubation compared to selenate sample can be explained by the increased production of proteins necessary for selenite reduction and nanoparticle stabilization.

In addition, the selenite toxicity was tested by adding different selenite concentrations (1 mM, 2.5 mM, 5 mM) to the bacterial suspension and monitoring of their influence

on cell growth. Results indicate that an increase of selenite concentration further prolonged the lag-phase of growth: from 2 days for 1 mM selenite to 6 days for 2.5 mM and 5 mM selenite (data not shown). Afterwards, selenite reduction started slowly which could be seen by a change of culture color and determination of selenite concentration by HG-AAS. However, a definite lethal selenite concentration was not determined within the investigated concentration and time range. In general, results agree well with literature data from Tugarova et al. [32, 33] who described growth inhibition of *A. brasilense* up to 42 h of cultivation in presence of selenite concentrations up to 1 mM followed by a bacterial selenite reduction to elemental red selenium nanoparticles. For a concentration of 10 mM no growth was observed [32, 33]. Compared to other bacteria [17, 42] which tolerate higher selenite concentrations, *A. brasilense* is more sensitive to Se-toxicity and consequently exhibits a lower reduction rate.

In an additional experiment (supplementary data), the selenite reduction capability of *A. brasilense* in the two environmentally occurring waters Spree river water (SW; Sohland, Saxony, Germany) and mine water of Königstein (KW; Königstein, Saxony, Germany) supplemented with 1 mM selenite were investigated. The bacteria grew in both waters (Figure S 1) and were able to reduce selenite to 20% and 55% of the initial concentration within 9.5 days (Figure S 2) accompanied by the formation of selenium particles (Figure 3). The differences in the selenite reduction capability within these two waters can be attributed to the prolonged lag-phase in KW compared to SW which might be due to the higher heavy metal load in KW (e.g. U 13 mg/L, Pb 0.6 mg/L, Zn 4 mg/L). This first experiment shows the potential of microbial biotransformation of selenite for bio-remediation purpose.

3.2 Localization and structural characterization of the microbial formed selenium particles

Light microscopic observations of *A. brasilense* cultured in presence of selenate and selenite indicated that reduction of selenite leads to production of red selenium particles in the growth medium, whereas selenate had no visible effect on the cultures. A closer look on both bacterial suspensions with SEM (Figure2 A & B) confirmed the first impression, as no morphological changes of the bacteria in the presence of selenate or selenite were observed. However, the micrographs of the cultures grown in the presence of selenite demonstrate the formation of spherical extracellular particles (Figure 2B). This observation is in contrast to the mainly intracellular Se^0 particles seen by Tugarova et al. [32, 33] after the reduction of selenite by *Azospirillum brasilense*. Cell lysis can be an explanation for occurrence of extracellular particles [33]. In this study particles were never seen inside the cells and the observed number of extracellular particles and intact cells gives rise to the assumption that enzymatic reactions occurring next to the cell surface or in the surrounding medium are responsible for the selenite reduction. However, it cannot be ruled out that selenite reduction starts inside the cells followed by secretion of small particles (< 100 nm) which grow further outside the cells as described for *S. maltophilia* [19].

To minimize the biological interference for the chemical microanalysis by EDX, the formed particles were isolated from the biomass using a modified procedure following Oremland et al. [37]. Electron microscopy of the isolated particles (Figure 2C & D) confirmed the spherical shape in the nano-size range with a high morphological homogeneity.

EDX spectra of the spherical particles (Figure 2E) display the characteristic X-ray emission lines for selenium with peaks at 1.4 keV (Lα), 11.2 keV (Kα) and 12.5 keV (Kβ) [37]. Furthermore, signals for silicon, oxygen, copper and sulfur were detected.

While the silicon signal is caused by the substrate used for SEM sample preparation, the copper signal can be explained by fluorescence excitation of the TEM support grid. For TEM, silicon and oxygen are also detected next to the Se particles. The detection of sulfur indicates an involvement of sulfur into the formation of selenium particles. The majority of investigations concerning the microbial reduction of selenite to particular Se^0 postulated biologically formed pure Se nanospheres [17], which were structurally unique compared to elemental selenium formed by chemical synthesis [37]. However, globules with a mixed sulfur–selenium content have been described by Nelson et al. [43] for sulfur-accumulating bacterium *Chromatium vinsosum*.

Raman spectroscopy was used to verify a possible formation of selenium–sulfur particles by *A. brasilense*. Spectra recorded at wavenumbers from 200 to 550 cm^{-1} provided a direct characterization of the structure of the molecular unit in $Se_{8-n}S_n$ mixed crystals [44]. The Raman spectrum of the isolated particles is characterized by two bands, where the band at 257 cm^{-1} can be assigned to the symmetric bond-stretching mode of a Se chain [45] and the second band at 356 cm^{-1} to S–Se stretching vibrations [44]. In comparison with the Raman spectra published by Eysel and Sunder [44], who studied a homologous series of various Se_nS_{8-n} mixed crystal compounds, this data corresponds excellently to the spectrum of the Se_6S_2 species. Similar to literature, the spectrum is only characterized by the stretching vibration of Se–Se and S–Se interactions. Furthermore, the typical S-S stretching band ($\approx$ 450 cm^{-1}) is missing in the Raman spectrum, which would be correlated with high sulfur content in the mixed crystals. In addition to the results from EDX microanalysis, the Raman data clearly confirm the biogenesis of selenium–sulfur particles by *A. brasilense*.

The selenite reduction experiments conducted in two environmental waters (supplementary data) and the characterization of the formed isolated spheres with STEM-EDX (Figure 3) suggest that the formation of the nanoparticles with mixed selenium-sulfur content strongly depends on the available sulfur concentration. In case of low sulfate concentration (≤ 300 mg/L) in Spree river water (SW), the EDX spectrum (Figure 3D) of the biogenically formed spheres displays the characteristic X-ray emission lines for selenium suggesting pure selenium nanoparticles. In contrast, at high sulfate concentration (850 mg/L) in mine water of Königstein (KW), the additional presence of the sulfur emission line at 2.3 keV (Kα) in the EDX spectrum of Figure 3C suggests mixed selenium-sulfur particles. These results in natural waters are in good agreement with the formation of selenium–sulfur particles in the Azo-Medium with a sulfate concentration of 800 mg/L.

To clarify the oxidation state of the Se particles formed by microbial reduction of selenite in the growth medium and for verification of sulfur contribution to the particle formation, XAS was performed. An X-ray Absorption Near Edge Structure (XANES) edge energy of 12656 eV as well as the overall shape of the white line and post-white line features confirm the zero-valent oxidation state of the *A. brasilense* Se nanoparticle sample (NP) (Figure 4A, Table 1) [46].

The Fourier transform magnitude (Figure 4B) shows the typical strong backscattering peak from the two coordinating Se neighbors of the 8-rings typical for red (amorphous) Se^0. In comparison to a red Se^0 standard, the peak is shifted to slightly lower R and has a lower amplitude. This is reflected (cf. Table 1) by the fitted Se-Se distance of 2.34 Å, i.e. 0.02 Å shorter than the reference, and a higher static disorder (σ^2 of 0.0035 $Å^2$ in comparison to 0.0025 $Å^2$ for the reference). Both features are in

line with a partial S-for-Se substitution in the 8-rings. A fit with an additional Se-S shell, however, failed.

Table 1: Se-K edge XANES edge energies and EXAFS fit data.

Sample	E/eV	Path	CN	R/Å	σ^2/Å^2	ΔE^0/eV	%R
A. brasilense NP's	12655.9	Se-Se	2.2	2.34	0.0036	7.7	2.9
Red Se^0	12656.1	Se-Se	2.2	2.36	0.0025	12.6	0.8

3.3 Size and physical properties of the microbial formed $Se_{8-n}S_n$ structured particles

The size of the isolated particles could be estimated from the electron micrographs, but for a statistically significant determination of the particle size distribution PCS measurements were conducted. Isolated particles formed by *A. brasilense* within two experiments showed a particle size ranging from 200 to 800 nm. The majority of the particles have a diameter of around 400 nm (Figure 5).

So, the observed particle size range in our study was larger than the one reported for various other microorganisms [17, 18, 32, 33, 37] typically ranging from 150 nm to 400 nm. If the definition of nanoparticle is adhered strictly, particle size would be limited to 100 nm or smaller [47]. Hence, the microbially produced selenium-sulfur particles in this study are better classified as submicron particles.

In another experiment, mean particle size in dependence on cultivation time was investigated. Therefore, during two cultivations of *A. brasilense* with selenite, samples were taken after different time intervals, particles were subsequently isolated and afterwards investigated by PCS. As shown in Figure 6, at the 3rd day of cultivation, the particles had a smaller mean diameter with 200 nm compared to the

particles formed for the rest of the investigated time characterized by a size of 330 nm.

So, particle growth under the investigated conditions is limited somehow, although the availability of selenite was still given with around 60% of initial amount left after 6 days of *A. brasilense* cultivation (Figure 1). The limitation in particle size might be due to presence of extra polymeric substances (EPS), capping the Se-S particles [36, 48]. Jain et al. [48] suggested that a larger size of some EPS-capped Se particles might be due to sub-optimal EPS-to-elemental Se ratio during formation of Se nanoparticles. The increase in particle size up to day 6 could be explained by a non-sufficient amount of potential capping polymers. Than with further increase in biomass (Figure 1) the amount of available capping polymers increased to a sufficient quantity compared to existing elemental selenium particles which lead to stopping growth of Se particles.

Further characterization of the Se-S particles was done by zeta potential measurements over a pH-range from 1 to 7. Figure 7 shows that the surface charge of the Se-S particles is negative over the whole investigated pH range. Starting with -3 mV at pH 1, the zeta potential decreased down to -18 mV at pH 7.

As the microbial reduction of selenite occurred while the pH shifted from 7.5 to 9.5, it is obvious that the Se-S particle formation and stabilization was favored by the high negative surface charge [17]. The negative surface charge can be attributed to organics (e.g. proteins, carbohydrates, extracellular polymeric substances – EPS) [48] covering the selenium particles. The recently published study of Kamnev et al [36] proofed biopolymers like proteins, polysaccharides and lipids to be associated with Se particles formed by *Azospirillum brasilense.* Additionally, a negative zeta-potential of -21 to -24 mV for another *A. brasilense* strain was mentioned in this study. The

negative ζ-potential value of the Se-S nanoparticles at pH values below 5.5 indicates a contribution of a large number of carboxylic acid groups to the covering organic layer [48]. This organic cover is clearly a result of bacterial metabolism as chemically formed Se^0, e.g. by reduction of selenite with hydroxylamine in the used *A. brasilense* medium without bacteria, tends to form amorphous aggregates with a rapid sedimentation [37]. However, the $Se_{8-n}S_n$ containing spheres showed long-time stability of some months in Milli-Q water and slow sedimentation as they repel each other as a result of the highly negative surface charge [17, 49]. The colloidal properties of selenium nanoparticle suspensions will also influence their environmental fate and the bioremediation effectiveness. Regarding the colloidal stability, the particles described in this study with a maximum ζ-potential of -18 mV are in between the colloidal stable (< -30 mV) and destabilized (< -15 mV) state [49]. This might be due to the presence of a monovalent counter cation, Na^+ (0.1 M NaCl), during the ζ-potential measurement and is in good agreement with values reported in literature under those conditions [48, 49]. So, for bioremediation purpose and modelling of migration behavior of Se^0 particles in natural waters, the pH as well as presence of counter cations and dissolved organic matter have to be taken into account for a reliable prediction of colloidal stability and settling behavior caused by particle agglomeration [49].

4. Conclusions

Azospirillum brasilense belongs to the group of bacteria able to reduce selenite under aerobic conditions to extracellular spherical $Se_{8-n}S_n$ structured particles in the submicron range. These results suggest that *Azospirillum* as a plant growth promoting rhizobacterium may help to prevent accumulation of selenium in crops cultivated on selenium-contaminated soils. Nevertheless, the cells are sensitive to the toxicity of

selenite as indicated by the growth profiles showing a prolonged growth lag-phase in presence of selenium. Because of this, an application of *Azospirillum* for remediation of selenium-contaminated water and soil in general is possible, but other bacterial strains, less sensitive to selenite and also able to reduce selenate, might be more useful.

The structure of the formed spherical particles is to our knowledge unique as there are no reports about bacteria forming Se particles containing a certain amount of sulfur. Comparison with Raman literature data suggests the formation of Se_6S_2 containing particles, but the amount of incorporated sulfur might vary depending on the cultivation conditions (e.g. sulfate concentration in medium or environmental water). Once formed, the $Se_{8-n}S_n$ structured particles are stable over several months as (destabilized) colloidal suspension because of the negative surface charge. For treatment of selenium-contaminated wastewater and migration behavior of selenium in the environment, this colloidal stability is unfavorable. As the particles occur extracellularly, they will not be entrapped in the biomass, do not settle fast enough as the surface charge leads to repulsion of the particles, and by this, selenium remains mobile to a certain amount although being less toxic.

Future studies are required to investigate the mechanism of aerobic microbial selenite reduction by *Azospirillum.* This is important to gain control over the biosynthesis, size, structure and stability of the particles considering their applications in nanobiotechnology, medicine as well as for the estimation of the migration of selenium through the environment in the context of risk assessment for the final disposals of nuclear waste.

Acknowledgements

The authors thank the beamline team at ROBL (ESRF Grenoble, France) for assistance during the XAS-measurements, the analytics group for elemental analysis and Stephan Weiß for assistance while nanoparticle characterization. Support by the Structural Characterization Facilities Rossendorf at IBC is gratefully acknowledged. This research did not receive any specific grant from funding agencies in the public, commercial, or not-for-profit sectors.

References

[1] D.L. Sparks, Environmental soil chemistry, 2nd ed., Academic Press, Burlington, 2003.
[2] F. Gore, J. Fawell, J. Bartram, Too much or too little? A review of the conundrum of selenium, J Water Health, 8 (2010) 405-416.
[3] A. Fernandez-Martinez, L. Charlet, Selenium environmental cycling and bioavailability: a structural chemist point of view, Rev Environ Sci Biotechnol, 8 (2009) 81-110.
[4] A. Olin, B. Noläng, E.G. Osadchii, L. Öhman, E. Rosen, Chemical Thermodynamics of Selenium. Chemical Thermodynamics Vol. 7
OECD Nuclear Energy Agency, Elsevier, 2005.
[5] D.R. Lide, CRC Handbook of chemistry and physics, 86th edn, 2005–2006, CRC Press, Boca Raton, 2005.
[6] H.J. Wen, J. Carignan, Reviews on atmospheric selenium: Emissions, speciation and fate, Atmos Environ, 41 (2007) 7151-7165.
[7] D. de Souza Mp, M. Chu, A.M. Zhao, S.E. Zayed, D. Ruzin, N. Schichnes, Terry, Rhizosphere bacteria enhance selenium accumulation and volatilization by indian mustard, Plant Physiol, 119 (1999) 565-574.
[8] H. Ohlendorf, D. Hoffman, M. Saiki, T. Aldrich, Embryonic mortality and abnormalities of aquatic birds: Apparent impacts of selenium from irrigation drainwater, Sci. Total Environ., 52 (1986) 49-63.
[9] G. Jörg, R. Buhnemann, S. Hollas, N. Kivel, K. Kossert, S. Van Winckel, C.L.V. Gostomski, Preparation of radiochemically pure Se-79 and highly precise determination of its half-life, Appl. Radiat. Isot., 68 (2010) 2339-2351.
[10] ONDRAF/NIRAS, Technical overview of the SAFIR 2 report. Safety Assessment and Feasibility Interim Report 2. NIROND 2001-05E, in, 2001.
[11] ANDRA, Synthèse: Evaluation de la faisabilité du stockage géologique en formation argileuse., in: Dossier 2005 Argile, 2005.
[12] C.I. Pearce, R.A.D. Pattrick, N. Law, J.M. Charnock, V.S. Coker, J.W. Fellowes, R.S. Oremland, J.R. Lloyd, Investigating different mechanisms for biogenic selenite transformations: *Geobacter sulfurreducens*, *Shewanella oneidensis* and *Veillonella atypica*, Environ. Technol., 30 (2009) 1313-1326.

[13] G.F. Combs, C. Garbisu, B.C. Yee, A. Yee, D.E. Carlson, N.R. Smith, A.C. Magyarosy, T. Leighton, B.B. Buchanan, Bioavailability of selenium accumulated by selenite-reducing bacteria, Biol. Trace Elem. Res., 52 (1996) 209-225.
[14] C. Garbisu, T. Ishii, T. Leighton, B.B. Buchanan, Bacterial reduction of selenite to elemental selenium, Chem. Geol., 132 (1996) 199-204.
[15] P.A. Kenward, D.A. Fowle, N. Yee, Microbial selenate sorption and reduction in nutrient limited systems, Environ. Sci. Technol., 40 (2006) 3782-3786.
[16] N.S. Vinod Yadav, Ranjana Prakash, K.K. Raina, L.M. Bharadwaj and N. Tejo Prakash, Generation of Selenium Containing Nano-Structures By Soil Bacterium, Pseudomonas aeruginosa, Biotechnology, 7 (2008) 299-304.
[17] S. Dhanjal, S.S. Cameotra, Aerobic biogenesis of selenium nanospheres by *Bacillus cereus* isolated from coalmine soil, in: Microb. Cell. Fact., 2010.
[18] M. Bajaj, S. Schmidt, J. Winter, Formation of Se (0) nanoparticles by *Duganella* sp and *Agrobacterium* sp. isolated from Se-laden soil of north-east Punjab, India, in: Microb. Cell. Fact., 2012.
[19] S. Lampis, E. Zonaro, C. Bertolini, D. Cecconi, F. Monti, M. Micaroni, R.J. Turner, C.S. Butler, G. Vallini, Selenite biotransformation and detoxification by *Stenotrophomonas maltophilia* SeITE02: Novel clues on the route to bacterial biogenesis of selenium nanoparticles, J Hazard Mater, 324, Part A (2017) 3-14.
[20] B. Huang, J. Zhang, J. Hou, C. Chen, Free radical scavenging efficiency of nano-Se in vitro, Free Radic Biol Med., 35 (2003) 805-813.
[21] J. Zhang, H. Wang, X. Yan, L. Zhang, Comparison of short-term toxicity between Nano-Se and selenite in mice, Life Sci, 76 (2005) 1099-1109.
[22] J.-S. Zhang, X.-Y. Gao, L.-D. Zhang, Y.-P. Bao, Biological effects of a nano red elemental selenium, BioFactors, 15 (2001) 27-38.
[23] Y. Bai, F.X. Rong, H. Wang, Y.H. Zhou, X.Y. Xie, J.W. Teng, Removal of copper from aqueous solutions by adsorption on elemental selenium nanoparticles, J. Chem. Eng. Data, 56 (2011) 2563-2568.
[24] T. Chen, Y.S. Wong, W. Zheng, Y. Bai, L. Huang, Selenium nanoparticles fabricated in *Undaria pinnatifida* polysaccharide solutions induce mitochondria-mediated apoptosis in A375 human melanoma cells, Colloid Surf. B-Biointerfaces, 67 (2008) 26-31.
[25] G. Blackburn, T.G. Scott, I.S. Bayer, A. Ghosh, A.S. Biris, A. Biswas, Bionanomaterials for bone tumor engineering and tumor destruction, J. Mater. Chem. B, 1 (2013) 1519-1534.
[26] Y. Huang, L. He, W. Liu, C. Fan, W. Zheng, Y.S. Wong, T. Chen, Selective cellular uptake and induction of apoptosis of cancer-targeted selenium nanoparticles, Biomaterials, (2013) 7106-7116.
[27] P.A. Tran, T.J. Webster, Antimicrobial selenium nanoparticle coatings on polymeric medical devices, in: Nanotechnology, 2013.
[28] S.A. Wadhwani, U.U. Shedbalkar, R. Singh, B.A. Chopade, Biogenic selenium nanoparticles: current status and future prospects, Appl Microbiol Biotechnol, 100 (2016) 2555-2566.
[29] R. Jain, D. Dominic, N. Jordan, E.R. Rene, S. Weiss, E.D. van Hullebusch, R. Hübner, P.N.L. Lens, Preferential adsorption of Cu in a multi-metal mixture onto biogenic elemental selenium nanoparticles, Chem. Eng. J., 284 (2016) 917-925.
[30] R. Jain, N. Jordan, D. Schild, E.D. van Hullebusch, S. Weiss, C. Franzen, F. Farges, R. Hübner, P.N.L. Lens, Adsorption of zinc by biogenic elemental selenium nanoparticles, Chem. Eng. J., 260 (2015) 855-863.

[31] S. Jiang, C.T. Ho, J.-H. Lee, H.V. Duong, S. Han, H.-G. Hur, Mercury capture into biogenic amorphous selenium nanospheres produced by mercury resistant *Shewanella putrefaciens* 200, Chemosphere, 87 (2012) 621-624.
[32] A.V. Tugarova, E.P. Vetchinkina, E.A. Loshchinina, A.G. Shchelochkov, V.E. Nikitina, A.A. Kamnev, The ability of the rhizobacterium *Azospirillum brasilense* to reduce selenium(IV) to selenium(0), Microbiology, 82 (2013) 352-355.
[33] A.V. Tugarova, E.P. Vetchinkina, E.A. Loshchinina, A.M. Burov, V.E. Nikitina, A.A. Kamnev, Reduction of selenite by *Azospirillum brasilense* with the formation of selenium nanoparticles, Microb. Ecol., 68 (2014) 495-503.
[34] R. Jain, M. Seder-Colomina, N. Jordan, P. Dessi, J. Cosmidis, E.D. van Hullebusch, S. Weiss, F. Farges, P.N.L. Lens, Entrapped elemental selenium nanoparticles affect physicochemical properties of selenium fed activated sludge, J Hazard Mater, 295 (2015) 193-200.
[35] M. Lusa, M. Bomberg, H. Aromaa, J. Knuutinen, J. Lehto, The microbial impact on the sorption behaviour of selenite in an acidic, nutrient-poor boreal bog, J. Environ. Radioact., 147 (2015) 85-96.
[36] A.A. Kamnev, P.V. Mamchenkova, Y.A. Dyatlova, A.V. Tugarova, FTIR spectroscopic studies of selenite reduction by cells of the rhizobacterium *Azospirillum brasilense* Sp7 and the formation of selenium nanoparticles, in: J. Mol. Struct., 2016.
[37] R.S. Oremland, M.J. Herbel, J.S. Blum, S. Langley, T.J. Beveridge, P.M. Ajayan, T. Sutto, A.V. Ellis, S. Curran, Structural and spectral features of selenium nanospheres produced by Se-respiring bacteria, Appl Environ Microb, 70 (2004) 52-60.
[38] N. Jordan, A. Ritter, A.C. Scheinost, S. Weiss, D. Schild, R. Hübner, Selenium(IV) uptake by maghemite (gamma-Fe_2O_3), Environ. Sci. Technol., 48 (2014) 1665-1674.
[39] S.M. Webb, SIXpack: a graphical user interface for XAS analysis using IFEFFIT, Phys. Scripta, T115 (2005) 1011-1014.
[40] T. Ressler, WinXAS: a program for X-ray absorption spectroscopy data analysis under MS-Windows, J. Synchrotron Radiat., 5 (1998) 118-122.
[41] A.L. Ankudinov, B. Ravel, J.J. Rehr, S.D. Conradson, Real-space multiple-scattering calculation and interpretation of x-ray-absorption near-edge structure, Phys. Rev. B, 58 (1998) 7565-7576.
[42] A. Ghosh, A.M. Mohod, K.M. Paknikar, R.K. Jain, Isolation and characterization of selenite- and selenate-tolerant microorganisms from selenium-contaminated sites, World Journal of Microbiology & Biotechnology, 24 (2008) 1607-1611.
[43] D.C. Nelson, W.H. Casey, J.D. Sison, E.E. Mack, A. Ahmad, J.S. Pollack, Selenium uptake by sulfur-accumulating bacteria, Geochim. Cosmochim. Acta, 60 (1996) 3531-3539.
[44] H.H. Eysel, S. Sunder, Homonuclear bonds in sulfur-selenium mixed-crystals - A Raman spectroscopic study, Inorg. Chem., 18 (1979) 2626-2627.
[45] V.V. Poborchii, A.V. Kolobov, H. Oyanagi, S.G. Romanov, K. Tanaka, Structure of selenium incorporated into nanochannels of mordenite: dependence on ion exchange and method of incorporation, Chem. Phys. Lett., 280 (1997) 10-16.
[46] A.C. Scheinost, R. Kirsch, D. Banerjee, A. Fernandez-Martinez, H. Zaenker, H. Funke, L. Charlet, X-ray absorption and photoelectron spectroscopy investigation of selenite reduction by Fe-II-bearing minerals, J. Contam. Hydrol., 102 (2008) 228-245.
[47] P. Borm, D. Robbins, S. Haubold, T. Kuhlbusch, H. Fissan, K. Donaldson, R. Schins, V. Stone, W. Kreyling, J. Lademann, J. Krutmann, D. Warheit, E.

Oberdorster, The potential risks of nanomaterials: a review carried out for ECETOC, in: Part. Fibre Toxicol., 2006, pp. 11.
[48] R. Jain, N. Jordan, S. Weiss, H. Foerstendorf, K. Heim, R. Kacker, R. Hübner, H. Kramer, E.D. van Hullebusch, F. Farges, P.N.L. Lens, Extracellular polymeric substances govern the surface charge of biogenic elemental selenium nanoparticles, Environ. Sci. Technol., 49 (2015) 1713-1720.
[49] B. Buchs, M.W.H. Evangelou, L.H.E. Winkel, M. Lenz, Colloidal properties of nanoparticular biogenic selenium govern environmental fate and bioremediation effectiveness, Environ. Sci. Technol., 47 (2013) 2401-2407.

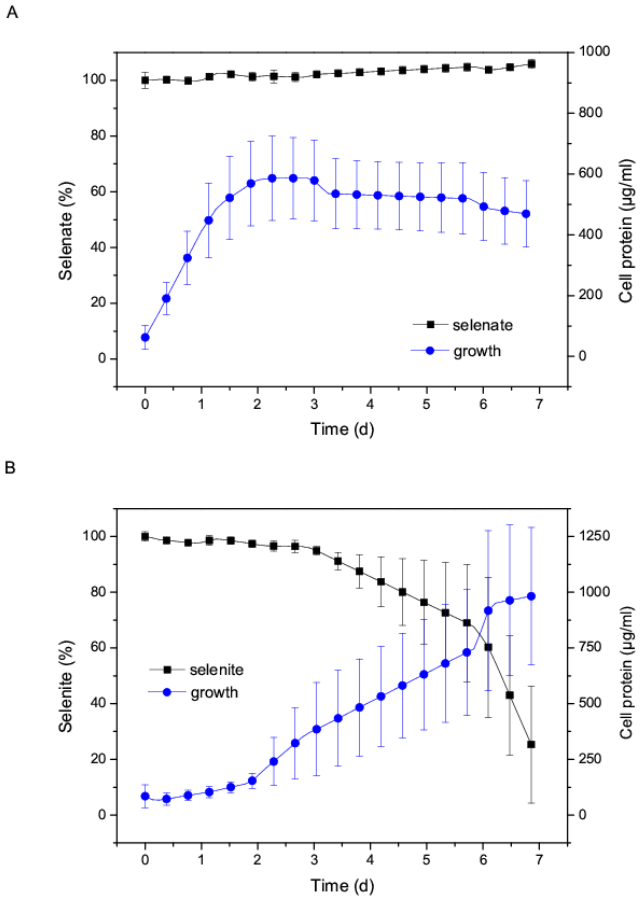

Figure 1: Growth profiles of *A. brasilense* and corresponding selenate (A) and selenite (B) concentration in percent of initial applied 1 mM. Average values of four selenate and three selenite experiments and corresponding standard error are given.

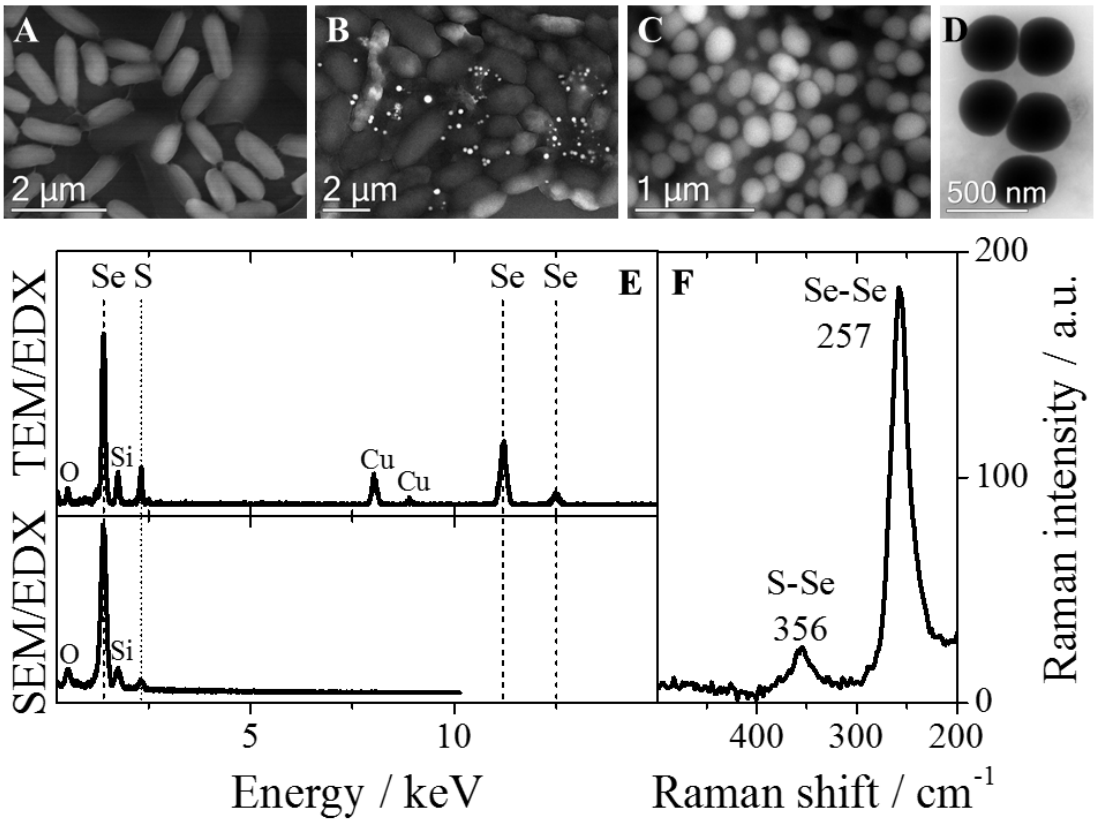

Figure 2: : Micrographs of Azospirillum brasilense and Se particles (A-D) with corresponding EDX (E) and Raman spectra of isolated Se particles (F). SEM image of *A. brasilense* with 1 mM selenate (A) and 1 mM selenite (B), SEM and TEM image of isolated Se particles (C & D).

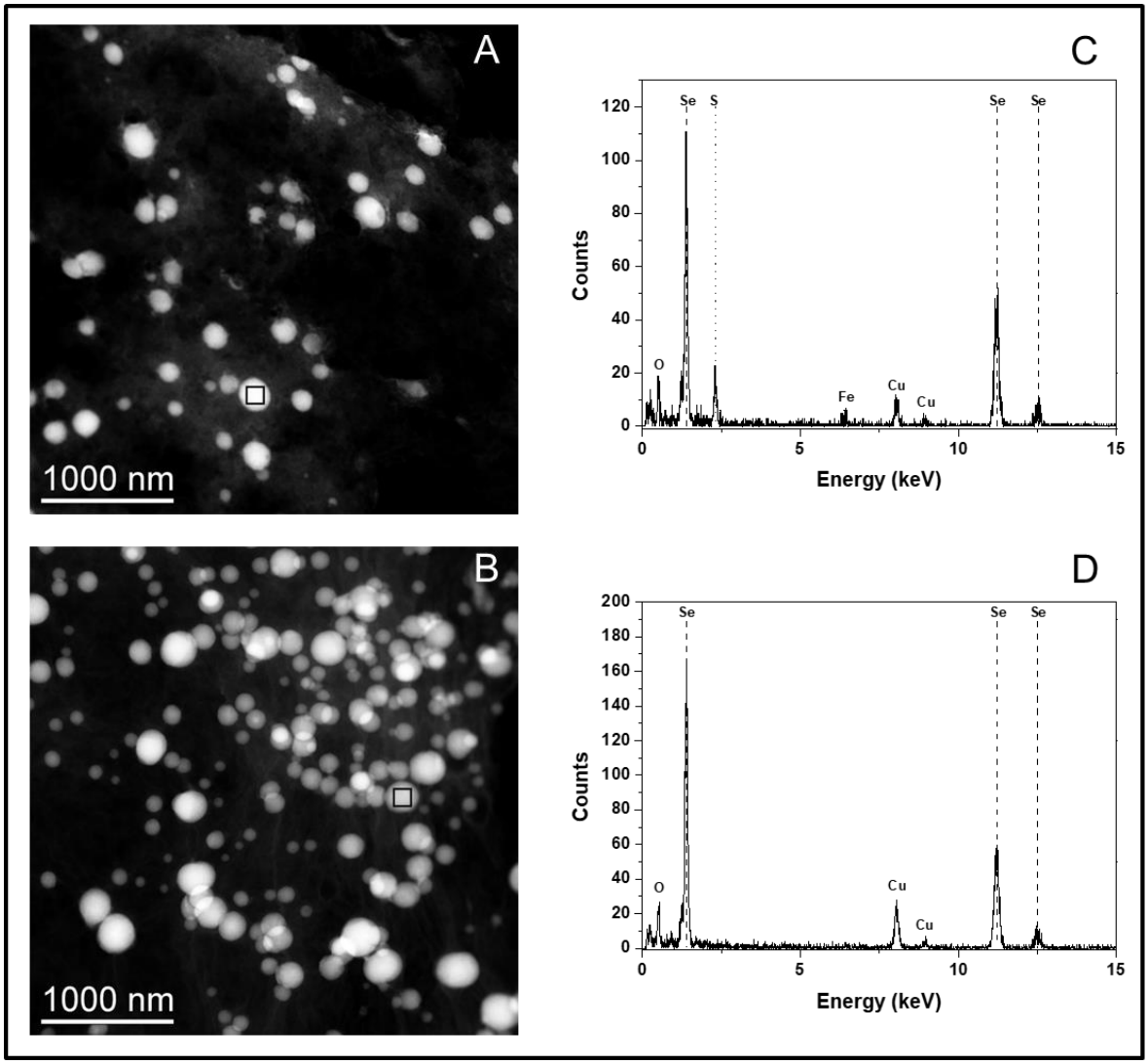

Figure 3: High-angle annular dark-field scanning TEM micrographs of isolated Se particles (A-B) with corresponding EDX spectra (C-D) obtained from the regions marked with a black square. Particles were biogenically formed by *A. brasilense* in environmental waters with differing sulfate concentrations supplemented with 1 mM selenite. A & C: mine water from Königstein (KW) with 850 mg/L sulfate; B & D Spree river water (SW) with ≤ 300 mg/L sulfate.

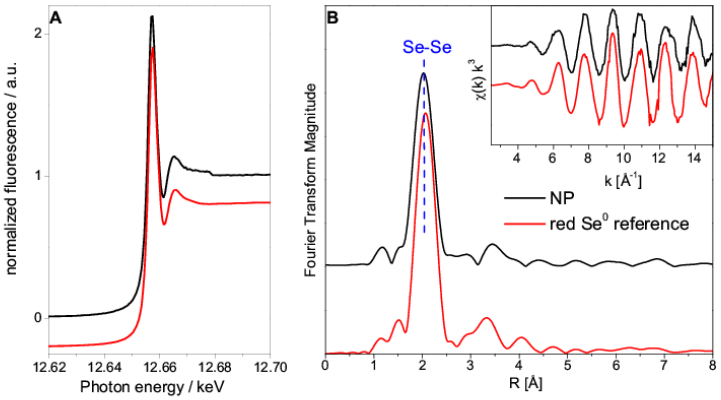

Figure 3: Se-K XAS spectra of microbially formed Se-S-particles. A: XANES, B: EXAFS Fourier Transform magnitude and k^3-weighted EXAFS spectra as insert.

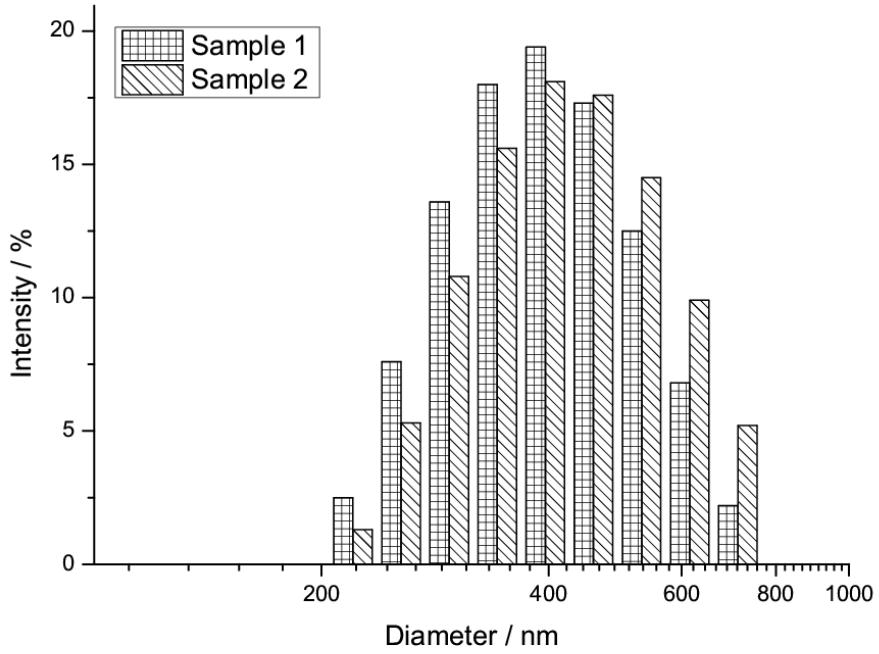

Figure 4: $Se_{8-n}S_n$ containing particle size distribution of two selenite reduction experiments determined with PCS.

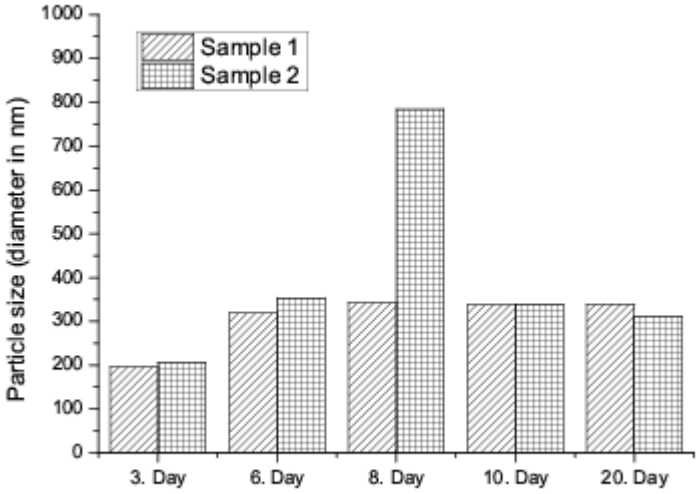

Figure 5: Mean $Se_{8-n}S_n$ particle size at different time points of bacterial growth in two identical selenite reduction experiments (1 mM).

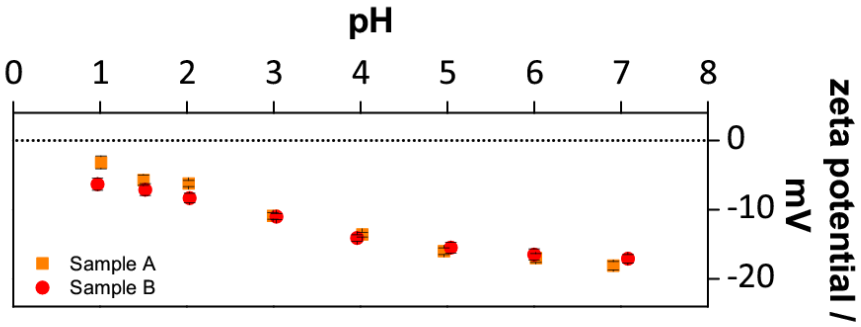

Figure 6: Zeta potential of $Se_{8-n}S_n$ particles (200 nm at pH 7.1) of two identical selenite reduction experiments (1 mM) as function of pH in 0.1 M NaCl solution.